

Influence of reduction process on the structure and properties of bismuth-silicate glasses

KONRAD TRZEBIATOWSKI, AGNIESZKA WITKOWSKA, TOMASZ KLIMCZUK

Department of Solid State Physics, Faculty of Technical Physics and Applied Mathematics, Technical University of Gdańsk, ul. Narutowicza 11/12, 80-952 Gdańsk, Poland.

We report on the investigations into the kinetics of hydrogen reduction process, and some other reduction-related phenomena in the $0.3 \text{ Bi}_2\text{O}_3 \cdot 0.7 \text{ SiO}_2$ glass. Use has been made of the various experimental methods, such as measurements of DC electrical conductivity, MIR, DSC and optical microscopy. The reduction process has been shown to lead to significant changes in the physical properties of the near-surface layer of glasses under consideration. The near-surface layer, originally dielectric, becomes semiconducting. Within the reduced layer a granular structure appears. We suggest that the carrier transport might consist in thermally activated hops between localised centres, which are related to the reduction-induced structural defects.

1. Introduction

The structural role played by Bi_2O_3 in silicate glasses is complicated and very poorly understood. It is not known exactly how, and to what extent, the presence of bismuth oxide influences mechanical, optical, and electrical properties of these glasses. Numerous experiments suggest that bismuth cations, in the presence of H_2 molecules, and at suitably chosen temperature, can undergo a reduction process, and thus become neutral atoms (similarly as Pb, Ar or Sb cations) [1], [2]. This process is accompanied by an increase of the electrical conductivity [3]. Moreover, the diffusion of neutral bismuth atoms in the matrix leads to their coalescence into metallic granules [4], [5].

In the present paper we report on our investigations on the kinetics of hydrogen reduction, and on some other reduction-related phenomena in the $0.3 \text{ Bi}_2\text{O}_3 \cdot 0.7 \text{ SiO}_2$ glass. In our study, we used various experimental methods, including measurement of the DC electrical conductivity, MIR, DSC and optical microscopy.

The paper is organised as follows. Section 2 is dedicated to rather technical issues, such as sample preparation, and measuring techniques. In Section 3, we present the results of our experiments and a short discussion. Section 4 contains concluding remarks.

2. Experiment

2.1. Sample preparation

Bismuth-silicate glass composed of $0.3\text{Bi}_2\text{O}_3 \cdot 0.7\text{SiO}_2$ was synthesised as follows. The mixture of powdered silica (SiO_2) and bismuth nitrate ($4\text{BiNO}_3(\text{OH})_2 \cdot \text{BiO}(\text{OH})$), placed in a platinum crucible, was gradually heated in an electrical furnace starting from the room temperature up to $800\text{ }^\circ\text{C}$. At this temperature, thermal decomposition of nitrate to oxide occurred, and a well phase-separated ceramal appeared. After milling the ceramal, a slow heating (3–4 hours) to $1200\text{ }^\circ\text{C}$ was performed. The melt was kept at the melting temperature for several minutes, being stirred mechanically in order to homogenise it. From the melt prepared in the way described one can produce samples in the form of rods, pastilles or powders.

2.2. Measurements

In order to investigate the DC conductivity, rods of diameter $d \approx 1.5\text{ mm}$ ($\Delta d \approx 10\text{ }\mu\text{m}$) and inter-electrode length l equal to 4 mm ($\Delta l \approx 0.1\text{ mm}$) were used. Such rods were equipped with two doubly coiled wire electrodes (constantan, $\varnothing = 0.1\text{ mm}$), placed in cuts near their ends. Electrical contact was provided by colloidal graphite. The conductivity measurements were performed in a special quartz chamber (for details, see [6]). Powdered samples (grain diameter $\leq 20\text{ }\mu\text{m}$) were used for IR and DSC measurements. The IR spectra in the range of $400\text{--}2000\text{ cm}^{-1}$ were collected using the IFS66 Bruker spectrometer. The DSC measurements were performed in the temperature range from $-100\text{ }^\circ\text{C}$ to $600\text{ }^\circ\text{C}$ at the scanning rate of 10 deg/min .

3. Results and discussion

3.1. Surface conductivity

Figure 1 presents temporal changes of surface conductivity σ of the $0.3\text{Bi}_2\text{O}_3 \cdot 0.7\text{SiO}_2$ glass during the hydrogen reduction process. One can distinguish the following stages of the conductivity variations. During the first stage (1 in Fig. 1) only a slight increase of σ is observed. On further annealing in hydrogen atmosphere (stage 2) a rapid increase in conductivity is observed (by 5–6 orders of magnitude). For longer times σ still systematically increases (stage 3). Assuming that the underlying transport mechanism is the carrier hopping between localised centres, the said variations of surface conductivity might be interpreted as follows. During stage 1 dispersed defects (localised states) appear, so the carrier jumps become only slightly easier. During stage 2 the defect concentration increases so strongly that percolation paths are formed. A weak conductivity increase during stage 3 could be related to an increase in the thickness of the reduced surface layer.

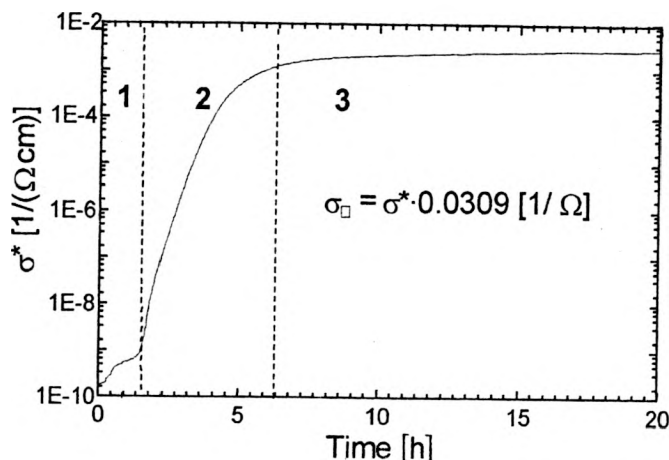


Fig. 1. Changes in surface conductivity of the $0.3\text{Bi}_2\text{O}_3 \cdot 0.7\text{SiO}_2$ glass during the hydrogen reduction process at $T = 300^\circ\text{C}$.

3.2. Mass losses during the reduction process

The reduction process of the near-surface layer of bismuth-silicate glasses consists in the chemical reaction of H_2 molecules of sufficiently high thermal energy with oxygen atoms bonded simultaneously to silicon and bismuth ions. The resulting H_2O molecules leave diffusively the sample, and are pumped out from the measurement chamber together with the working gas (hydrogen). After the reaction, the unsaturated silicon bonds can disappear in a number of relaxation processes, and weakly bonded bismuth atoms appear, which can migrate and agglomerate into metallic granules. The process described can be observed by measuring the sample mass loss during reduction. Such measurements performed during the reduction process, realised at various temperatures, can give much information on the process, and on the related changes of physical and structural properties of the layer being modified. The kinetics of the oxygen losses at two different temperatures (300 and 350°C) is shown in Fig. 2 (curves *a* and *b*, respectively). It is worth noting that: a) the mass losses are initially the linear functions of time, b) the rate of the mass loss in this time interval is temperature-dependent, c) the total mass-loss of oxygen co-ordinated to bismuth atoms from completely reduced samples is identical for both temperatures (about 50%, statistically this means that only one half of all oxygen atoms co-ordinating bismuth atoms takes part in the reaction).

The linearity of the mass changes permits us to determine the activation energy for the chemical reaction going on during the annealing in hydrogen atmosphere. In particular, using the Eyring formula

$$u = \frac{kT}{h} \exp\left(-\frac{\Delta E_a}{kT}\right)$$

where u is the reaction rate, h is the Planck constant, k is the Boltzmann constant, and E_a is the free energy of activation of the process (barrier height), one obtains the values shown in Fig. 2.

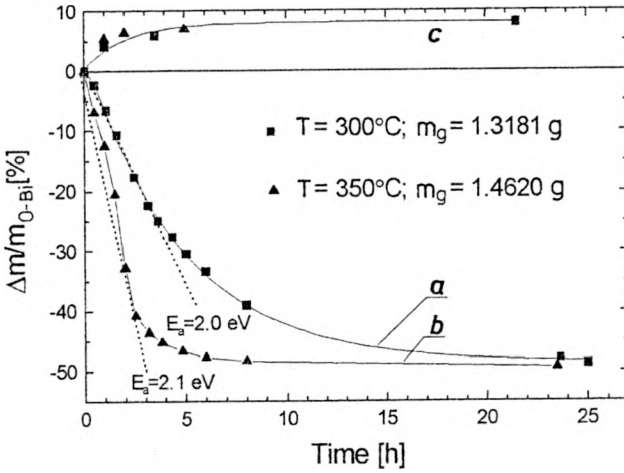


Fig. 2. Changes in sample mass during the reduction (curves *a* and *b*) and annealing in the oxygen atmosphere (curve *c*): m_g — total mass of oxygen within the sample, m_{O-Bi} — total mass of oxygen co-ordinating bismuth atoms.

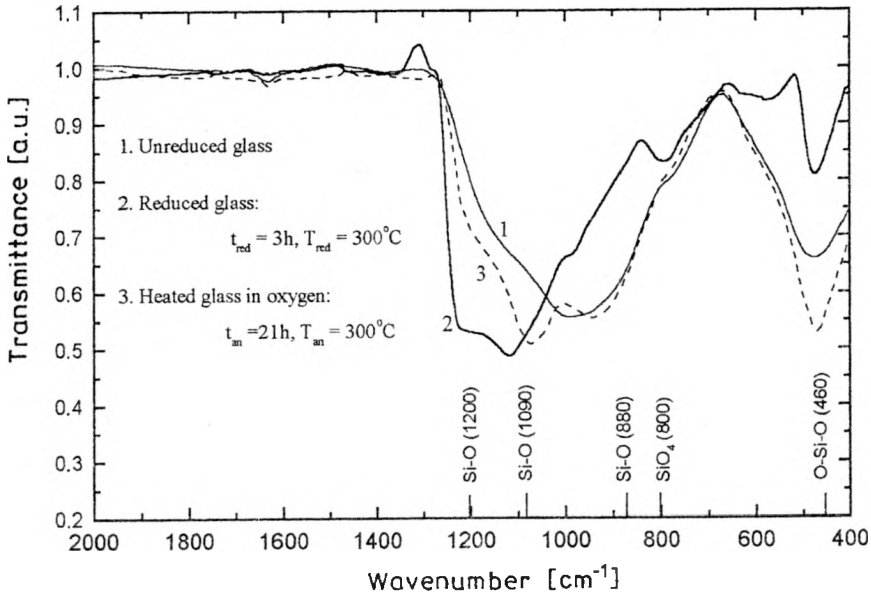


Fig. 3. IR spectra: 1 — unreduced glass, 2 — reduced glass, 3 — reduced glass additionally submitted to the annealing process in oxygen atmosphere. The parameters of reduction and annealing processes are given in the figure.

Figure 2 shows also an increase in the mass of totally reduced samples annealed in the oxygen atmosphere (curve *c*). The mass increase is related to oxidation of the glass and saturation of the Si ions. The latter effect is presented in Fig. 3, where the IR spectra for unreduced, reduced, and reduced-annealed in the oxygen atmosphere samples, are compared. On oxygen annealing the glass structure begins to resemble the structure of pure amorphous silica, at least as far as the Si–O bond vibrations are concerned.

3.3. Properties of the reduction front

Figure 4 shows cross-sections of partially reduced grains as viewed by the optical reflection microscope. The grains were submitted to a 72 hours' reduction process at 300 °C. Figure 4a shows reduced grains, left for several days in ambient atmosphere at room temperature. The inner part of the reduced layer is covered with small drops of water. The strong tendency to adsorb water molecules from air can be explained assuming the existence of unsaturated bonds in this region. Figure 4b shows similar grains, which have been well relaxed by prolonged annealing in vacuum prior to the several-day exposition to ambient atmosphere in the same conditions as samples from Fig. 4a. No water adsorption is observed. The latter fact suggests that the continuous tetrahedra network is reconstructed in the relaxation processes.

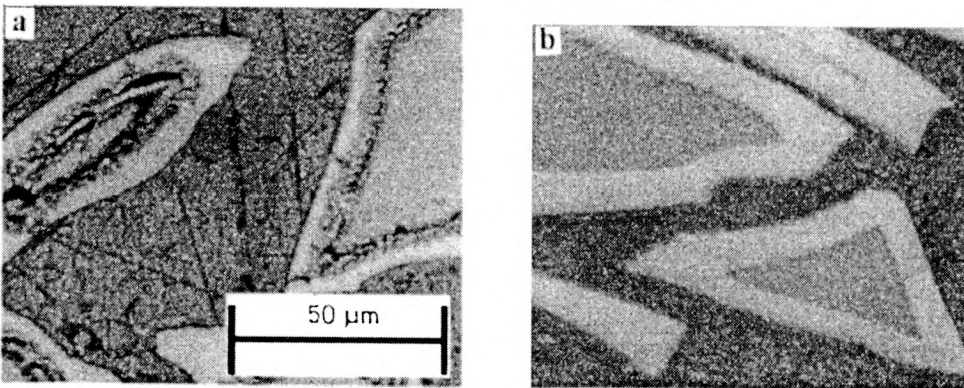


Fig. 4. Optical microscope images of powdered glass grains. Dark inner part – unreduced part of glass, bright outer part – reduced surface layer: **a** – after the reduction process (droplets of water are clearly seen on the boundary between unreduced and reduced parts), **b** – after the reduction and annealing process (no water droplets).

The appearance of a distinct boundary between the external reduced layer and the central unreduced part of the grains (so well seen in the reflected light, Fig. 4) is related to the structural changes induced by the reduction process. The reduced glass is in fact a silica glass (see Fig. 3), in which nano-structured metallic bismuth phase is contained (the unreduced glass is homogeneous).

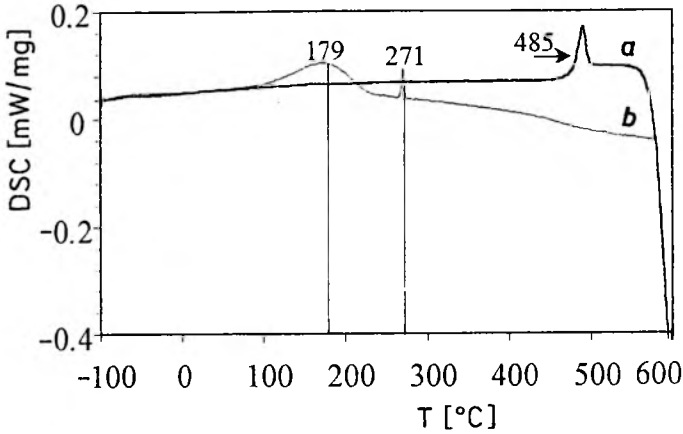


Fig. 5. Results of DSC measurement: *a* – unreduced glass, *b* – reduced glass ($T_{\text{red}} = 300\text{ }^{\circ}\text{C}$, $t_{\text{red}} = 65\text{ h}$).

thermic peak related to glass transition ($T_g = 485\text{ }^{\circ}\text{C}$), and strong variations above $550\text{ }^{\circ}\text{C}$, related to the crystallisation (exothermic) process. On the other hand, in the case of a reduced glass, the heat uptake curve has a sharp maximum at $270\text{ }^{\circ}\text{C}$, related to the melting of on-surface bismuth granules [5], and a wide endothermic peak in the temperature range from $100\text{ }^{\circ}\text{C}$ to $200\text{ }^{\circ}\text{C}$, related to the melting of bismuth structures immersed in the glass. A significant width of the latter peak

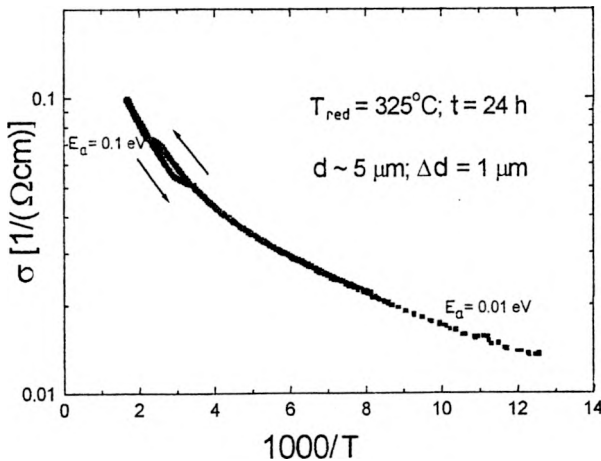


Fig. 6. Conductivity of reduced glass during the cooling and heating processes (the parameters of the reduction are given in the figure).

suggests a wide distribution of sizes of the confined bismuth structures. Gradual decrease of the heat uptake for $T > 200\text{ }^{\circ}\text{C}$ results from the structural relaxation process. The appearance of the metallic phase in the silica matrix can also be seen on the electrical conductivity curve. The hysteresis (Fig. 6) can be related to the melting and solidification of the nano-sized bismuth granules embedded in the SiO_2 network.

4. Conclusions

It has been shown that the reduction process leads to significant changes in the physical properties of the near-surface layer of glasses under investigation. The near-surface layer, originally dielectric, becomes semiconducting. It seems probable that the carrier transport consists in thermally activated hops between localised centres, which are related to the reduction-induced structural defects. In reduced glass a granular structure appears.

Acknowledgements – The work was partially supported by the Polish State Committee for Scientific Research (KBN), grant No. 7 T08D 027 19.

References

- [1] MIYAJI F., YOKO T., JIN J., *et al.*, *J. Non-Cryst. Solids* **175** (1994), 211.
- [2] TUZZOLO M.R., SHELBY J.E., *J. Non-Cryst. Solids* **143** (1992), 181.
- [3] TRZEBIATOWSKI K., WITKOWSKA A., CHYBICKI M., *Ceramics* **57** (1998), 157.
- [4] WITKOWSKA A., RYBICKI J., MANCINI G., FELIZIANI S., *Ceramics* **57** (1998), 147.
- [5] CZAJKA R., TRZEBIATOWSKI K., POLEWSKA W., *et al.*, *Vacuum* **48** (1997), 213.
- [6] TRZEBIATOWSKI K., KUSZ B., WITKOWSKA A., *et al.*, [In] The 1st National Conference: *Material Engineering* (in Polish), May 25–26, 2000, Gdańsk (Poland), p. 234.

Received September 18, 2000